Vol-06 Issue 05, May -2022 ISSN: 2456-9348
Impact Factor: 5.004

iJETRM
International Journal of Engineering Technology Research & Management

PSO BASED PID CONTROL FOR EXCITATION SYSTEM OF LARGE SYNCHRONOUS MOTOR

Hung Quoc Duong[*1]
Dung Thi To[2]
[*1]Faculty of Electrical Engineering, Thai Nguyen University of Technology, Vietnam
[2]Faculty of civil and environment, Thai Nguyen university of Technology, Viet Nam

ABSTRACT
This paper proposes a PID controller, using the particle swarm optimization (PSO) algorithm to optimize control parameters. The control object is an excitation system for a large synchronous motor, which is widely used in large power transmission systems. In practice, the change in load and excitation source can affect the operating mode of the motor. Therefore, the controller is designed to stabilize the power factor, resulting in better working performance. Initially, the controller is designed based on the Ziegler–Nichols method, then the PSO optimization algorithm is used to optimize the controller parameters. Numerical simulation results demonstrate the advantage of the proposed approach.

Keyword:
Synchronous Motor; Excitation system; Particle swarm optimization; PID Controller.

1. INTRODUCTION
Synchronous motors have apparent advantages in efficiency, torque, and operational stability. Therefore, it is widely utilized in large power transmission systems. The power factor correction of high-power synchronous motors is helpful in applications where the motor is subjected to high transient load variations. This power factor is measured and sent to the controller; a control signal is then calculated and sent to the thyristor static rectifier to adjust the value of the excitation source supplied to the rotor winding of the motor. Accordingly, the traction torque of the synchronous motor is adjusted during transient load [1-2]. In addition, the power controller recognizes the voltage drop of the power grid within a certain allowable period to provide a solution to adjust the field current accordingly [3-4]. Another application of power factor correction is to control plant power factor variations caused by other loads such as asynchronous motors running under or without load, thereby improving the voltage quality of the plant [5-6]. Therefore, stabilizing the value of the power factor will indirectly stabilize the operating mode of the motor.

PID is a controller proposed by [7] and it has become a widely used tool in industry. Determining the PID controller parameters can be done by different methods, in which Ziegler-Nichols [8] is a very effective method when the mathematical model is not required to be known [9 - 11]. The combined Ziegler-Nichols and trial and error method have refined the accuracy of the controller parameters [12-15]. In [15], a PI controller is designed to excite the rotor of the synchronous motor to track the power factor setpoint. This method further refines the controller parameters and achieves better results than that using only Ziegler-Nichols. In [16], the experience of operators is used to adjust the PID controller parameters. In the steady-state, the above studies show that the response still has relatively large fluctuations.

The design of the PID controller and the adjustment of the coefficients is simple, especially for linear objects. For nonlinear systems, however, the PID controller becomes inefficient. To solve this problem, optimization algorithms are proposed, such as particle swarm optimization [17-18]. Compared with mathematical algorithms and other

iJETRM
International Journal of Engineering Technology Research & Management

heuristic optimization techniques, PSO is simple, easy to implement, robust to control parameters, and has computational efficiency. In this study, PSO is proposed to optimize the parameters of the PID controllers to adjust the power factor in the excitation control system of the synchronous motor.

The main contributions of this work include (i) the critical analyze the effect of load and excitation source to the operating mode of synchronous motor, and (ii) the PID schemes using PSO algorithm to achieve a stable power factor.

The rest of this paper is structured as follows. The problem description is given in Section 2. Section 3 describes the control design, and Section 4 presents simulation results. Finally, a conclusion is provided in Section 5.

2. PROBLEM DESCRIPTION

2-1- Excitation system of large synchronous motor

For a large synchronous motor, the power supply to the stator is usually a medium voltage grid, 6kV. The excitation source for the motor is usually a low voltage grid, 380V, which is lowered to the appropriate voltage level through a rectifier transformer. This power supply is then rectified to direct current to supply excitation current to the motor. To stabilize the working mode of the motor, the power factor stabilization plays a crucial role. Therefore, an excitation controller is designed aiming to stabilize the power factor cosφ. The block diagram of the excitation control system for a synchronous motor is shown in Figure 1.

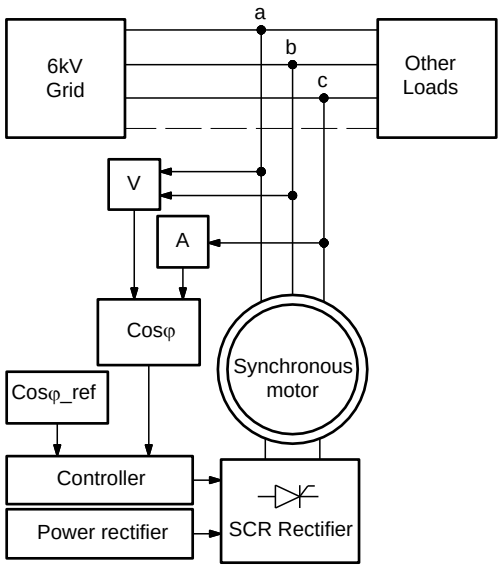

Figure 1. Block diagram of excitation control for synchronous motor.

The phase difference between voltage and current is measured and compared to a desired $cos\varphi$. The controller then calculates a control signal, which is sent to the rectifier to adjust the excitation current in order to achieve the desired power factor. To ensure favorable measurement of the phase difference between voltage and current, the stator windings of the synchronous motor can be star or delta connected to the grid. A typical power factor measurement method is to measure the angle of the voltage between two phases and the current of the other phase, as shown in Figure 2. The figure demonstrates that u_{ab} is 90^0 earlier earlier than u_c. Therefore, when calculating the phase difference angle between voltage and current, φ, the stator must shift the angle of u_{sab} by an angle of 90^0 to coincide with the angle of u_{sc}.

iJETRM
International Journal of Engineering Technology Research & Management

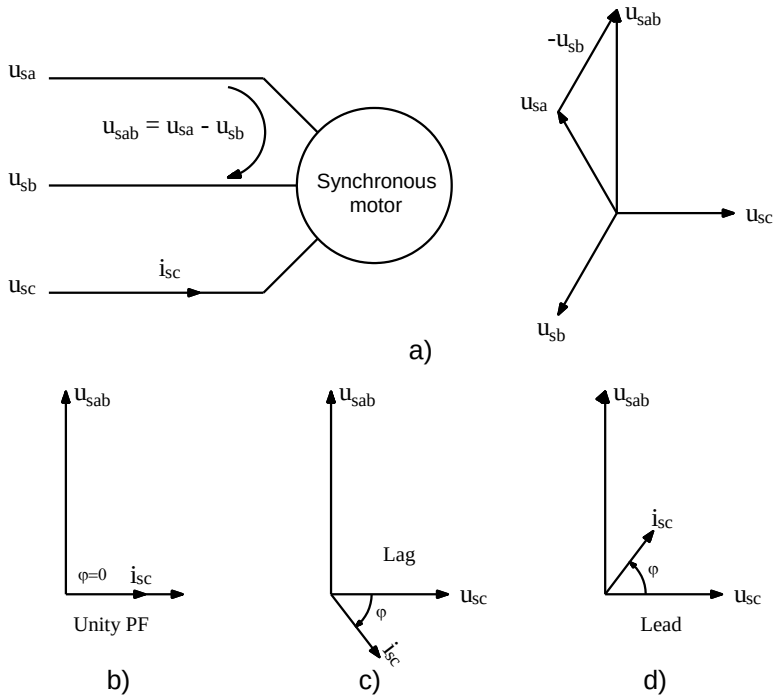

Figure 2. Vector diagram of stator current and voltage: (a) Vector diagram of stator current; (b) current and voltage are in same phase; (c) current lags behind voltage in phase; and (d) current leads ahead of voltage in phase.

2-2- Motor modelling

In this section, the backgrounds of the synchronous motor modelling are presented to demonstrate the critical role of power factor regulation and stabilization.

2-2-1-Motor equations and equivalent circuits

Figure 3 shows a two-axis salient pole synchronous motor in a rotor coordinate system. The frame for stator windings, (α, β), is stationary with the real axis attached to the stator phase A. Meanwhile, the frame for the excitation and the damper windings, (d, q), is rotating with the real axis fixed to the center of the pole shoe. This coordinate system rotates with the rotor angular velocity, so both d- and q- magnetic paths are constant. The excitation winding, (f), is attached on the the d-axis. The damper winding is replaced by two windings in space quadrature, one on the d- axis, (D), and the other on the q-axis (Q). The stator three-phase winding is also replaced by two windings in perpendicular space, on the d-axis, (d), and on the q-axis (q). The electrical equations of the motor are given as below [19]:

$$u_d = R_s i_d + \frac{d\psi_{sd}}{dt} - \omega_r \psi_{sq}, \quad (1)$$

$$u_q = R_s i_q + \frac{d\psi_{sq}}{dt} + \omega_r \psi_{sd}, \quad (2)$$

iJETRM
International Journal of Engineering Technology Research & Management

$$u_f = R_f i_f + \frac{d\psi_f}{dt}, \tag{3}$$

$$u_D = R_D i_D + \frac{d\psi_D}{dt} = 0, \tag{4}$$

$$u_Q = R_Q i_Q + \frac{d\psi_Q}{dt} = 0, \tag{5}$$

where u_d is the d-axis stator voltage, u_q is the q-axis stator voltage, u_f is the excitation voltage, u_D is the d-axis damper winding voltage, u_Q is the q-axis damper winding voltage, i_d is the d-axis stator current, i_q is the q-axis stator current, i_f is the excitation current, i_D is the d-axis damper winding current, i_Q is the q-axis damper winding current, ψ_d is the d-axis stator flux linkage, ψ_q is the q-axis stator flux linkage, ψ_f is the excitation flux linkage, ψ_D is the d-axis damper winding flux linkage, ψ_Q is the q-axis damper winding flux linkage, $\omega_r = \frac{d\theta}{dt}$ is the angular velocity between the rotor coordinates and the stationary reference frame α, β, θ_r is the angle between the rotor coordinates and the stationary reference frame.

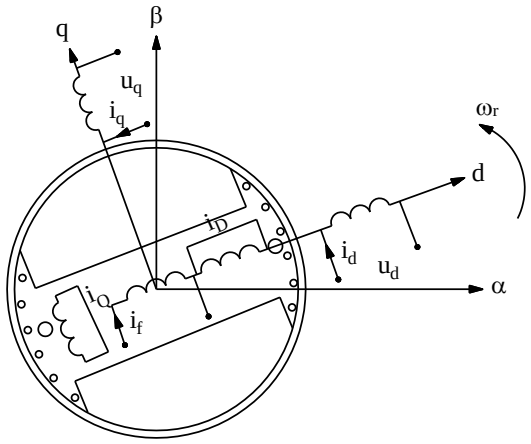

Figure 3. Two-axis salient pole synchronous motor model in the rotor coordinate systems.

The relationship between the motor currents and flux linkages can be defined by using various inductances of the motor [19]:

$$\psi_{sd} = \psi_{md} + i_d L_{s\sigma} = L_{md}(i_f + i_d + i_D) + i_d L_{s\sigma}, \tag{6}$$

$$\psi_{sq} = \psi_{mq} + i_d L_{s\sigma} = L_{mq}(i_q + i_Q) + i_q L_{s\sigma}, \tag{7}$$

$$\psi_f = \psi_{md} + i_f L_{f\sigma} + (i_f + i_D) L_{k\sigma} = L_{md}(i_d + i_D + i_f) + (i_f + i_D) L_{k\sigma} + i_f L_{f\sigma}, \tag{8}$$

$$\psi_D = \psi_{md} + i_D L_{D\sigma} + (i_f + i_D) L_{k\sigma} = L_{md}(i_d + i_D + i_f) + (i_f + i_D) L_{k\sigma} + i_D L_{D\sigma}, \tag{9}$$

iJETRM
International Journal of Engineering Technology Research & Management

$$\psi_Q = \psi_{mq} + i_Q L_{Q\sigma} = L_{md}(i_q + i_Q) + i_Q L_{Q\sigma}, \quad (10)$$

where L_{md} is the d-axis magnetising inductance, $L_{s\sigma}$ is the d-axis leakage inductance, $L_{D\sigma}$ is the d-axis damper winding leakage inductance, $L_{f\sigma}$ is the d-axis magnetising winding leakage inductance, $L_{k\sigma}$ is the d-axis Canay inductance, L_{mq} is the q-axis magnetising inductance, $L_{Q\sigma}$ is the q-axis damper winding leakage inductance, R_s is the stator resistance, R_f is the magnetising winding resistance, R_D is the d-axis damper winding resistance, and R_Q is the q-axis damper winding resistance.

From (1)–(10), the equivalent circuits of a synchronous motor can be obtained, as illustrated in Figures 4 and 5.

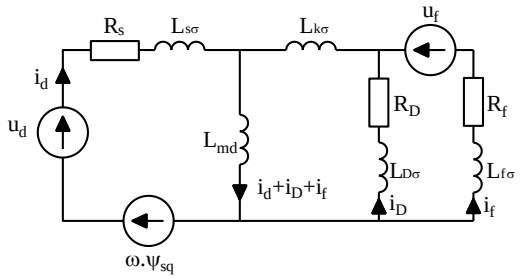

Figure 4. Equivalent circuits of the synchronous motor on the d- axis.

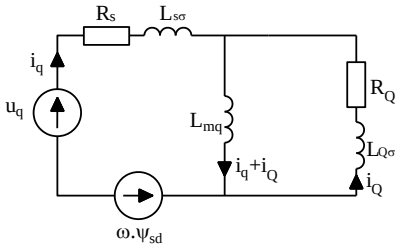

Figure 5. Equivalent circuits of the synchronous motor on the q- axis.

2-2-2-Vector diagram of a synchronous motor

From (1)–(10), the vector diagram of the salient pole synchronous motor is built as shown in Figure 6.

iJETRM
International Journal of Engineering Technology Research & Management

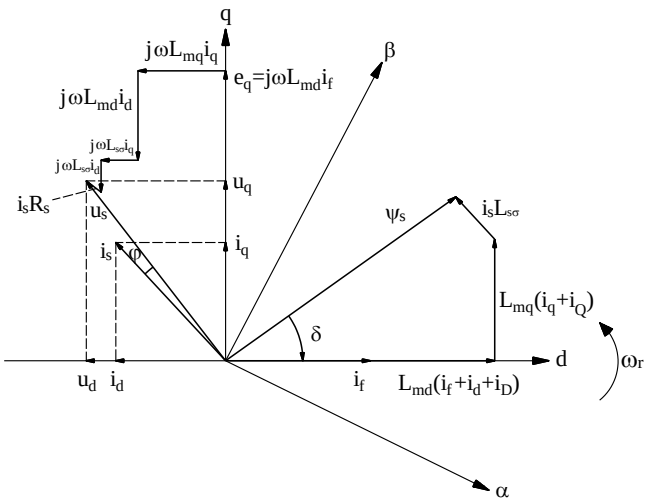

Figure 6. Vector diagram of the salient pole synchronous motor.

In fact, the stator resistance is usually minimal compared to its inductance. Therefore, the voltage drop across the stator resistor can be ignored. The total inductances in the machine are denoted as

$$L_{sd} = L_{s\sigma} + L_{md}, \tag{11}$$

$$L_{sq} = L_{s\sigma} + L_{mq}, \tag{12}$$

$$X_{sd} = \omega L_{sd}, \tag{13}$$

$$X_{sq} = \omega L_{sq}, \tag{14}$$

where X_{sd} and X_{sq} are corresponding d- and q-axis stator reactances. From (11), (12), and Figure 6, assuming that voltage drop on R_s is ignored, we obtain:

$$u_d = j(\omega L_{mq} + \omega L_{s\sigma})i_q = \omega L_{sq} i_q = jX_{sq} i_q, \tag{15}$$

$$u_q = e_q + j(\omega L_{md} + \omega L_{s\sigma})i_d = e_q + j\omega L_{sd} i_d = e_q + jX_{sd} i_d, \tag{16}$$

$$u_s = u_d + u_q = e_q + jX_{sd} i_d + jX_{sq} i_q = e_q + jX_s i_s, \tag{17}$$

where X_s is the stator reactance. From (15)–(17), a simplified vector diagram can be then constructed as shown in Figure 7, with the angle between the voltage vector, u_s, and the q-axis electromotive force, e_q, being the load angle δ.

iJETRM
International Journal of Engineering Technology Research & Management

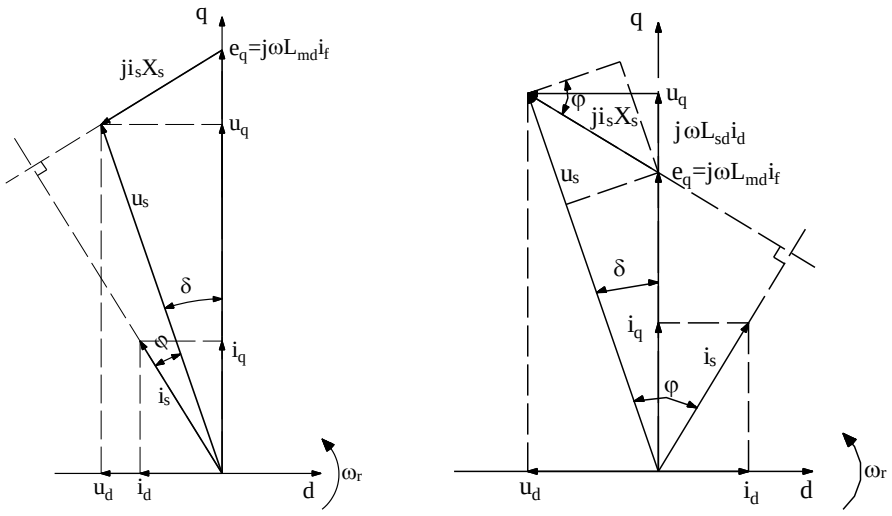

Figure 7. Vector diagramof a synchronousmotor in steady-statemodewhen statorwinding resistance is ignored, with $X_s = \omega L_s$: (a) Current leads of voltage in phase, and (b) Current lags behind voltage in phase.

According Figure 7b, we have:

$$I_sX_s\cos\varphi = E_q\sin\delta, \tag{18}$$

Accordingly,

$$U_sI_s\cos\varphi = \frac{U_sE_q\sin\delta}{X_s}. \tag{19}$$

where U_s and I_s are corresponding amplitude of stator voltage and current, E_q is the amplitude of excitation electromotive force, and $X_s = \omega L_s$ is the stator reactance.

The electromagnetic power of the motor, ignoring the losses, is given as below [20]:

$$P_e = P_m = \frac{3}{2}U_sI_s\cos\varphi\,, \tag{20}$$

where *Pe* and *Pm* are corresponding the electromagnetic power and motor power. From (19) and (20), we obtain:

$$P_e = P_m = \frac{3}{2}U_sI_s\cos\varphi = \frac{3}{2}\frac{U_sE_q\sin\delta}{X_s}. \tag{21}$$

Eq. (21) shows the relationship between power and excitation voltage and load angle. Assuming the source voltage and frequency are constant, we will have the following relationship:

$$P_e = P_m = f(I_s\cos\varphi), \tag{22}$$

$$P_e = P_m = f(E_q\sin\delta). \tag{23}$$

iJETRM
International Journal of Engineering Technology Research & Management

2-2-3-Torque equation of synchronous motor at steady state

From the vector diagram in Figure 7b, we have:

$$I_s \cos\varphi = I_q \cos\delta - I_d \sin\delta, \tag{24}$$

We can also compute:

$$I_d = \frac{U_q - E_q}{\omega L_{sd}} = \frac{U_s \cos\delta - E_q}{\omega L_{sd}}, \tag{25}$$

$$I_q = \frac{U_s \sin\delta}{\omega L_{sq}}. \tag{26}$$

Substituting (24)-(26) into (20), we obtain a second method to determine the electromagnetic power of the motor in working mode as:

$$P_e = \frac{3}{2}\frac{U_s E_q}{\omega L_{sd}}.\sin\delta + \frac{3}{2}U_s^2\frac{(L_{sd} - L_{sq})}{\omega L_{sd} L_{sq}}.\sin 2\delta. \tag{27}$$

The electromagnetic torque in working mode is calculated as:

$$T_e = \frac{P_e p_r}{\omega} = \frac{3p_r}{2\omega}[\frac{U_s E_q}{\omega L_{sd}}.\sin\delta + U_s^2\frac{(L_{sd} - L_{sq})}{\omega L_{sd} L_{sq}}.\sin 2\delta]. \tag{28}$$

Since ωL = X, (28) can be rewritten as:

$$T_e = \frac{3p_r}{2\omega}[\frac{U_s E_q}{X_{sd}}.\sin\delta + U_s^2\frac{(X_{sd} - X_{sq})}{X_{sd} X_{sq}}.\sin 2\delta]. \tag{29}$$

In the steady state, the electromagnetic torque of a salient pole synchronous motor has two components. The first part is the main synchronous torque, which depends on the AC voltage and excitation source, $U_s.E_q$. The second component is the reluctance torque which depends only on the stator voltage, U_s^2. Figure 8 depicts the torque–load angle characteristics of a salient pole synchronous motor, where $T_1(\delta)$ is the main synchronous torque, $T_1(\delta)$ is the reluctance synchronous torque, and $T_e(\delta)$ is the total synchronous torque.

From (29), torque regulation is critical so that the motor remains to work safely in the face of a voltage drop of the mains voltage or overload of the torque. To control the torque, we can adjust the field current, resulting in changing $T_1(\delta)$, which is the main synchronous torque.

iJETRM
International Journal of Engineering Technology Research & Management

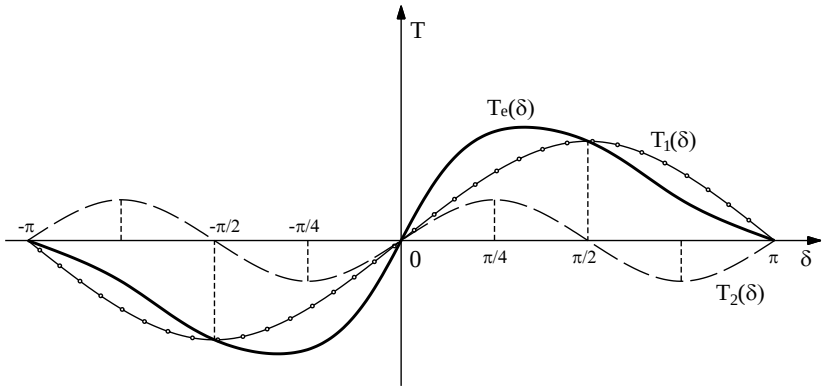

Figure 8. Torque–load angle characteristics of a salient pole synchronous motor.

2-3- Factors affecting the working mode of the motor

For a large synchronous motor, the fluctuation of the load in the operating mode can cause the load angle δ to change accordingly. An excessive change can cause an asynchronous phenomenon, i.e., the rotor magnetic pole slips from the stator magnetic pole. A change in the excitation source can also affect the operating mode of the motor. This section will discuss these effects, in which the load angle, δ, and the current-voltage phase difference, φ, are used to evaluate the operating mode of the motor.

2-3-1-Vector diagram of a synchronous motor

To make it easier to follow, we rotate the coordinate system of the vector diagram so that u_s coincides with the horizontal axis. Assume that the power supply, the power grid frequency, and the DC excitation source are constant. The vector diagram after rotation, in case of load change, is shown in Figure 9.

According to Figure 9, the motor is initially assumed to work with stator current i_{s1}, power αP_1, where α is a constant, power factor $\cos\varphi \approx 1$. When the load on the motor shaft increases to αP_2, the armature current will increase to the value i_{s2}. Assuming the excitation source is constant, its trajectory will draw an arc. Then, the phase difference angle φ increases in the positive direction, $\cos\varphi$ decrease, load angle increases, i.e., $\delta_2 > \delta_1$. When the load δ increases within a permissible range, the stator magnetic field can still lock the rotor magnetic field, so the motor speed remains unchanged. However, if the load increases sharply, δ_2 tends to go to -90^0. At this time, the motor is pulled out of synchronous mode. Therefore, the excitation controller must detect a decrease in the power factor to increase the field current to a suitable value to pull the motor into synchronous mode.

iJETRM
International Journal of Engineering Technology Research & Management

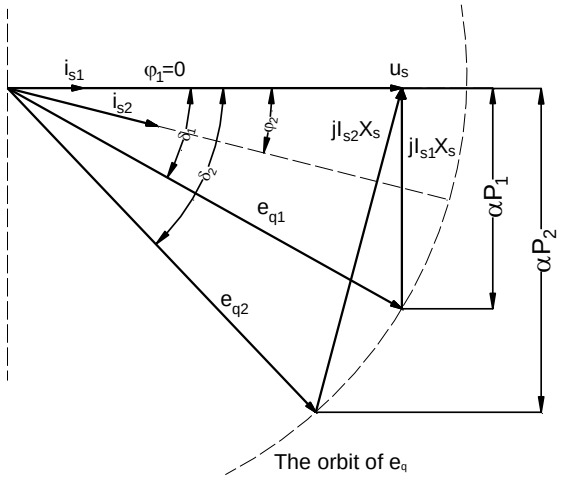

Figure 9. **Vector diagramof synchronousmotor when stator source and excitation source are constant, load changes from P_1 to P_2, with $P_2 > P_1$.**

2-3-2-The influence of the excitation source

From (21), if the load and AC source are fixed, then $E_q sin\delta$ is also a constant. Therefore, when increasing the excitation source E_q, the load angle will decrease. This causes the relative angular position between the rotor and stator magnetic fields to decrease, the stator magnetic poles will be more tightly attached to the rotor, and the motor will run at synchronous speed. The vector diagram when changing the excitation source value is illustrated in Figure 10, therein the subscript {1, 2, 3} are corresponding to three different excitation source values.

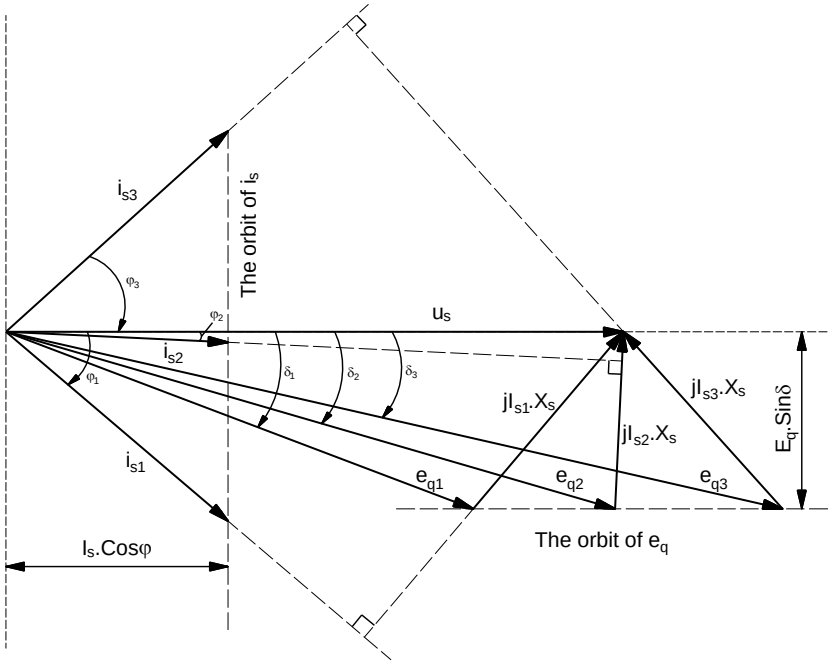

Figure 10. **The influence of the excitation source on the working mode.**

iJETRM
International Journal of Engineering Technology Research & Management

According to (21), with a fixed load, we have:

$$E_{q1}\sin\delta_1 = E_{q2}\sin\delta_2 = E_{q3}\sin\delta_3 = E_q\sin\delta. \quad (30)$$

From (30) and Figure 10 we see that the trajectory of E_q will slide parallelly to u_s.

Also, from (21), we have:

$$I_{s1}\cos\varphi_1 = I_{s2}\cos\varphi_2 = I_{s3}\cos\varphi_3 = I_s\cos\varphi. \quad (31)$$

From (31) and Figure 10 we see that the trajectory of i_s will slide perpendicular to u_s.

Increasing the excitation source from E_{q1} to E_{q3} causes the phase angle of the current with voltage to change from phase lag state to phase lead state. The value of the excitation source that produces the normal power factor is called the normal excitation. Excitement higher than the normal value is typically called over-excitation. In this scenario, the motor works as a synchronous compensator. Excitement lower than the normal value is called under-excitation. In this case, the engine works like an asynchronous machine. The above analysis shows that power factor correction is beneficial in applications where the motor is subjected to high transient loads. The power factor regulator must measure the power factor drop that occurs when the motor is subjected to a sudden heavy load and send a signal to the thyristor static rectifier to increase the value of the excitation source. This process is called excitation enhancement. As a result, the pull-out torque of the synchronous motor is increased during transient loads. After the load drops, the regulator senses the excessive lead-in power factor and drives the rectifier to drop the voltage at its output. Another application of the power factor regulator is to control the variation of the plant power factor caused by other loads such as asynchronous motor running under or no load, thereby improving the voltage quality of the plant.

3. PSO-BASED PID CONTROL DESIGN

3-1- PSO preliminaries

The PSO optimization algorithm, first proposed in [23], is a random search algorithm based on simulating the behavior and interaction of birds when looking for food sources. Each bird, called individual or element, in the flock, called population, is characterized by two components, the position vector x_i and the velocity vector v_i. Each individual has a fitness value, which is assessed by the fitness function. Initially, the PSO has initialized random position and velocity vectors. Then in each iteration of the algorithm, the velocity vector v_i and the position x_i of each individual will be updated as below:

$$v_i(k+1) = \omega(k)v_i(k) + c_1r_1(P_i(k) - x_i(k)) + c_2r_2(G(k) - x_i(k)), \quad (32)$$

$$x_i(k+1) = x_i(k) + v_i(k+1), \quad (33)$$

where k repesents the iteration; $\omega(k)$ is a weight parameter; c_1 and c_2 are corresponding cognitive and social parameter, r_1 and r_2 are random samples in the interval [0; 1]. At each iteration, each individual is influenced by the best position it has achieved, $P_i(k)$, and the global best position in all searches by all individuals in population, $G(k)$.

In this paper, PSO will be implemented to find the optimal parameters for a hybrid PID-FLC Sugeno control design for the excitation system of a large synchronous motor. The "particleswarm()" function in MATLAB software was used to perform the PSO algorithm.

3-2- PID control design for excitation system of large synchronous motor

The structure diagram of the excitation control system, using hybrid PID control, is shown in Figure 11. In this diagram, the object consists of a three-phase 6 pulse bridge rectifier and the synchronous motor. The output voltage of the rectifier will provide a field source for the rotor windings. The power factor $\cos\varphi$ is measured at the stator side

iJETRM
International Journal of Engineering Technology Research & Management

of the motor and compared with the setpoint. The error *e(t)* is fed to the PID controller for processing. The output signal of the PID controller is sent to the thyristor excitation regulator to change the DC output voltage of the rotor winding.

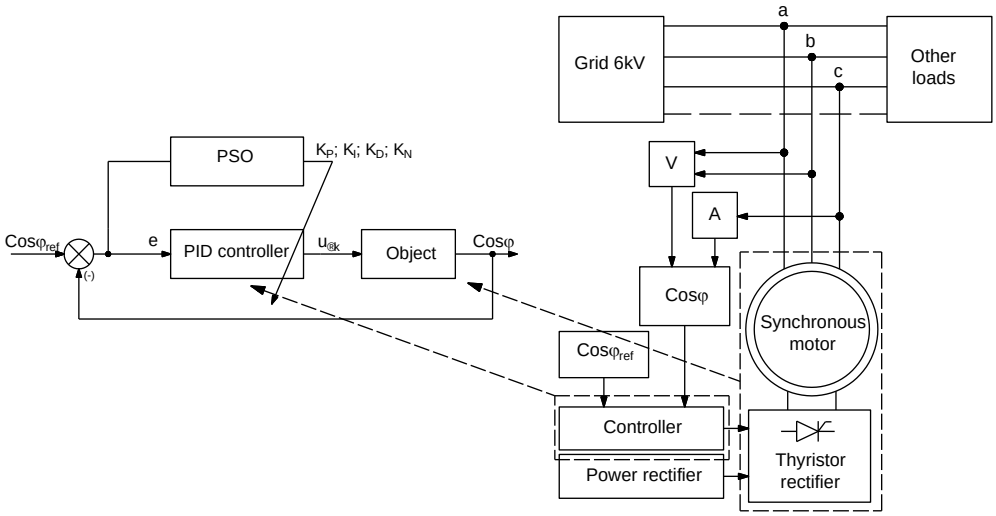

Figure 11. PSO-based PID controller

The feedback control signal is computed as

$$u(s) = e(s)\left[K_p + K_i\frac{1}{s} + K_d\frac{K_N}{1+K_N\frac{1}{s}}\right], \qquad (34)$$

where K_p, K_i , K_d are corresponding coefficients for proportional, integral, and derivative terms, K_N is the filter coefficient.

PID controller for synchronous motor excitation system, Initially, designed according to Ziegler-Nichols method. Then, the PSO swarm optimization control algorithm is used to optimize the controller parameter such as Kp; Ki; Kd and KN. The initialization domain for the PSO is taken around the parameter values found by the Ziegler-Nichols method above. The fitness function of the PSO is selected using the integral absolute error (IAE) index as below:

$$IAE = \sum_{k=1}^{n}|e(k)|, \qquad (35)$$

where *e(k)* is the error at *k*-iteration, *n* is the total number of samples in an iteration.

In the Matlab Toolbox, the *particleswarm()* function has been supported for optimization according to the PSO algorithm. In this paper, we use the existing *particleswarm()* function and follow the algorithm shown in Figure 12.

After running the PSO optimization program for the PID controller, the results are as follows: Kp = 0.549, Ki = 5.992, Kd = 0.5 and KN = 0.866.

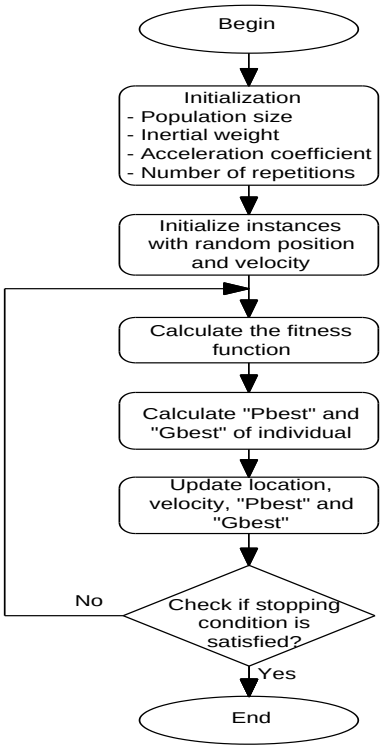

Figure 12. Flowchart of PSO

iJETRM
International Journal of Engineering Technology Research & Management

4. SIMULATION RESULTS

In this section, simulation is carried out on a convex pole synchronous motor working in a steady-state in the present load change. The simulation diagram on Matlab/Simulink using the psoposed PSO-based PID control system is shown in Figure 13. The simulation parameters are given in Table 1.

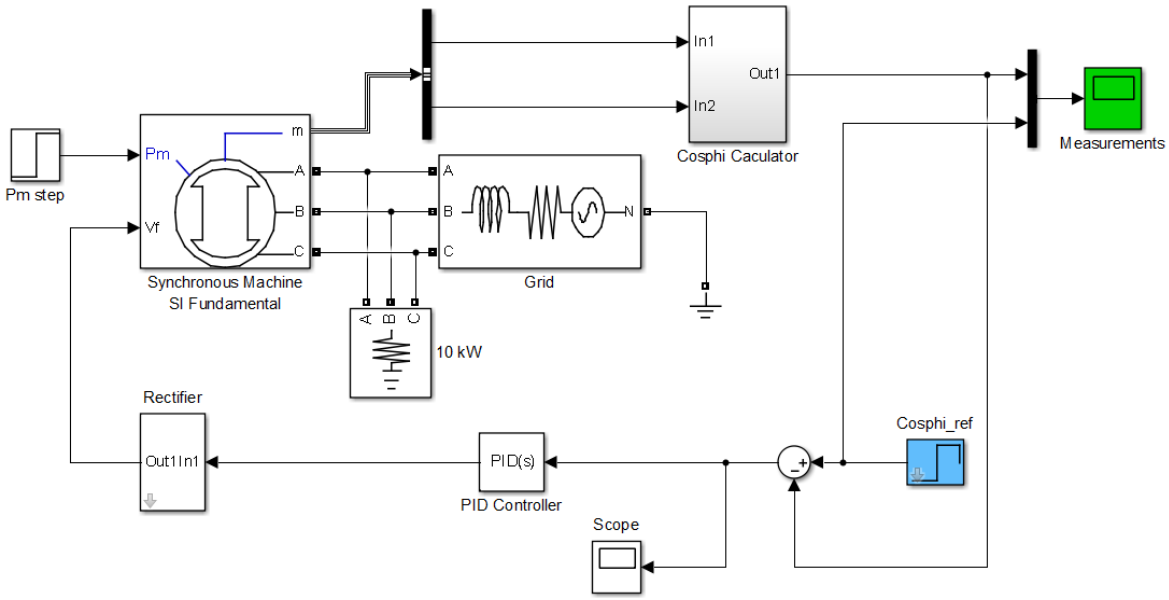

Figure 13. Control system on Matlab/Simulink

Table 1. An example of a table.

Parameter	Symbol	Value	Unit
Stator resistance	R_s	0.26	Ω
Stator leakage inductance	$L_{s\sigma}$	1.14	mH
d-axis magnetising inductance	L_{md}	13.7	mH
q-axis magnetising inductance	L_{mq}	11	mH
d-axis damper winding resistance	R_D	0.0224	Ω
d-axis damper winding leakage inductance	$L_{D\sigma}$	1.4	mH
q-axis damper winding inductanc	R_Q	0.02	Ω
q-axis damper winding leakage inductance	$L_{Q\sigma}$	1	mH
Number of pair of poles	p	10	-
Magnetising winding resistance	R_f	0.13	Ω
Magnetising winding leakage inductance	$L_{f\sigma}$	2.1	mH
Rate stator current of phase A	I_a	53.9	A
Rate Stator current of phase B	I_b	53.9	A
Rate Stator current of phase C	I_c	53.9	A
Initial phase A of the current	ph_a	-173.3	Degree

iJETRM
International Journal of Engineering Technology Research & Management

Initial phase B of the current	ph_b	66.7	Degree
Initial phase C of the current	ph_c	-53.3	Degree
Rate excitation source	E_q	57	V

To evaluate the quality of synchronous motor excitation control system, we compare the system response of the proposed PSO based PID to a PI controller. For the PI controller, K_p = 1 and K_i = 5 are selected using Ziegler-Nichols combined with trial and error method. For PID controller, Kp = 0.549, Ki = 5.992, Kd = 0.5 and KN = 0.866 are obtained by PSO algorithm. In the simulation, disturbance from the sudden increase of the added load, at t = 2.5s, causing the phase shift angle to change. The control system will automatically adjust the excitation source to stabilize the power factor *cosφ*.

To evaluate the quality of the excitation control system of the synchronous motor. We compare:

1. Using the PID controller, the controller parameters are determined by the Ziegler-Nichols.
2. Using the PID controller, controller parameters are determined by Ziegler-Nichols and Trial and error.
3. Using PID controller, controller parameters are optimized by PSO.

Figure 14 shows the simulation result when load is constant, the cosφ_ref is 0.85. PSO based PID controller gives the best quality, followed Ziegler-Nichols and Trial and error base PID controller, finally Ziegler-Nichols base PID controller.

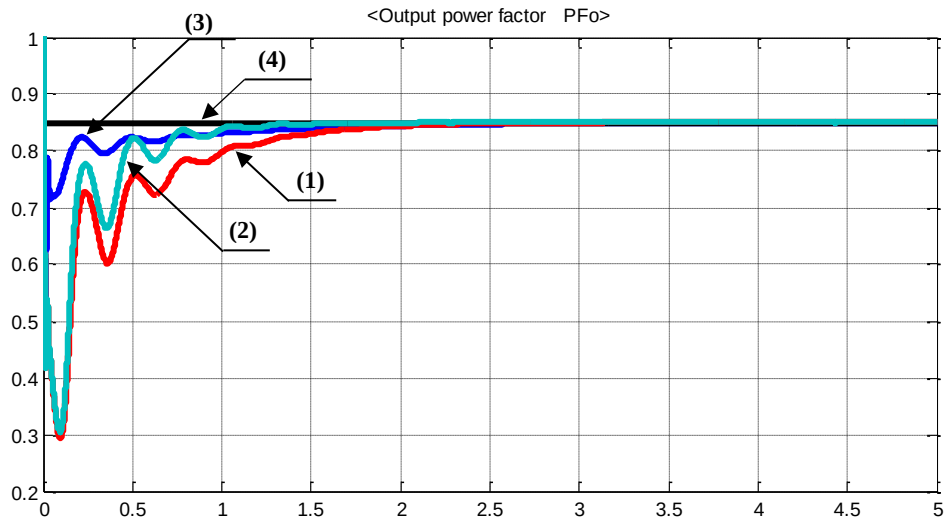

(1) Ziegler-Nichols base PID; (2) Ziegler-Nichols and Trial and error base PID; (3) PSO base PID; (4) cosφ_ref

Figure 14. Response of cosφ when cosφ_ref is 0.85

Figure 15 presents the response of the power factor when the load is increased at t = 3s with desired power factor *cosφ_ref* = 0.95. The figure demonstrates that all controllers present a quick response under the load change, where the PSO base PID controller presents slightly better performance than the others.

iJETRM
International Journal of Engineering Technology Research & Management

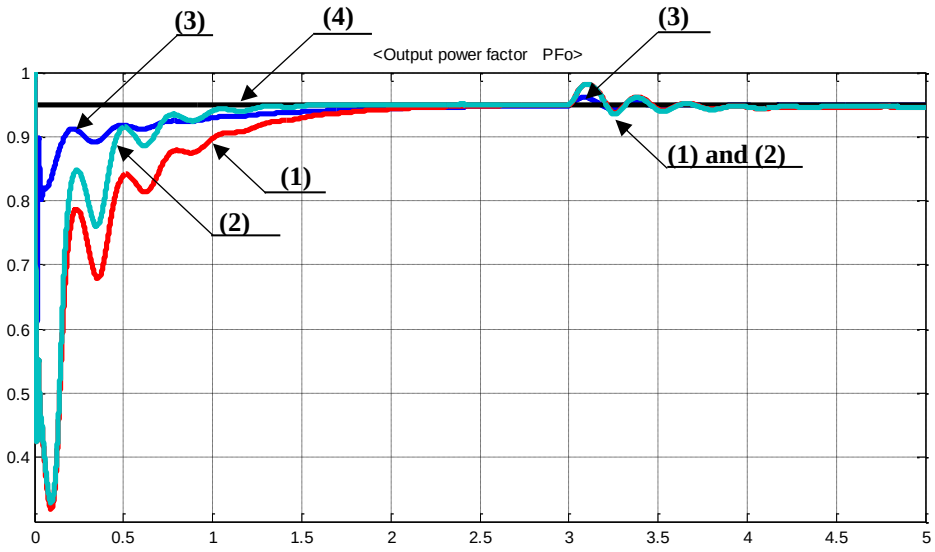

(1) Ziegler-Nichols base PID; (2) Ziegler-Nichols and Trial and error base PID; (3) PSO base PID; (4) cosφ_ref

Figure 15. Response of cosφ when cosφ_ref = 0.95 and load in increased 30% at t = 3s.

The above results show that using the PSO algorithmto optimize controller parameters of the PID controller for the excitation control system of a large-capacity synchronous motor in working mode is entirely feasible.

Figures 16 depicts values of IAE after each iteration of the proposed PSO algorithms. These figures illustrate that fitness functions converge to optimal values quickly, after about 11 iterations and best function value is 2.45 for PSO-based PID. More importantly, these figures show the advantages of the proposed approach.

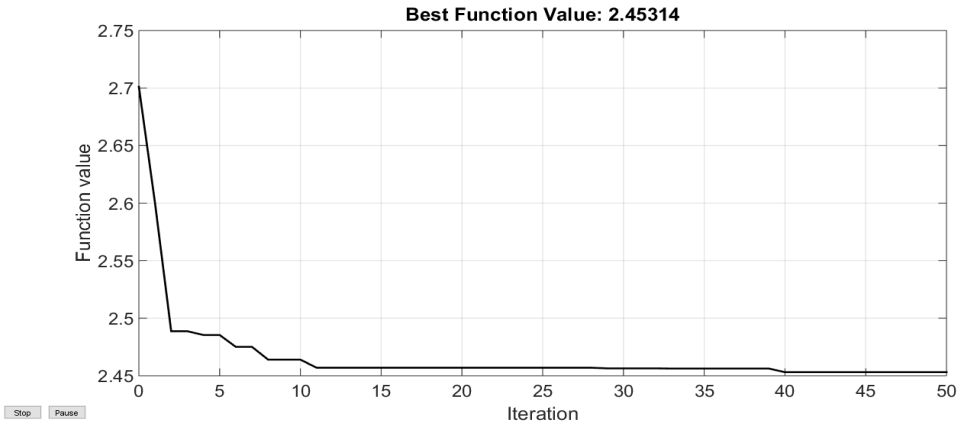

Figure 16. Fitness function of PSO algorithm to tune PID coefficients

5. CONCLUSION AND DISCUSSION

This manuscript introduced a PID controller for an excitation system of a large synchronous motor. The effect of load and excitation source on the motor's working mode is critically analyzed to demonstrate the importance of stabilizing the power factor. In the control system, the control parameters were optimized using the PSO algorithm.

iJETRM
International Journal of Engineering Technology Research & Management

The PSO is utilized to optimize the tuning coefficients K_p, K_i , K_d, and K_N of the PID controller. The simulation showed that the proposed controller presents the best control performance among the considered approaches. In our future works, the proposed algorithm will be applied to practical large power transmission systems and other reference tracking control applications.

DATA AVAILABILITY

Data sharing not applicable: No new data were created or analyzed in this study. Data sharing is not applicable to this article.

REFERENCES

[1] D P Kothari and I J Nagrath. “Electric machine.” TMH Publishers second edition (1998).
[2] M. G. Say. “Performance and design of ac machine.” CBS Publishers third edition (2002).
[3] DR. P.S. Bimbrha. “Electrical Machinery.” Khanna Publisher seventh edition (2009).
[4] Bill Horvath. “Synchronous Motors & Sync Excitation Systems.” Western Mining Electrical Association; TM GE Automation Systems (2009).
[5] Al-Hamrani MM, Jouanne AV, Wallace A. “Power factor correction in industrial facilities using adaptive excitation control of synchronous machines.” Conference Record of the 2002 Annual Pulp and Paper Industry Technical Conference, Toronto, Canada (June 2002).
[6] WEG group. “The ABC’s of Synchronous Motors.” At https://www.electricmachinery.com/_files/LR10012.gb.01-11.01_SynchMotors_Mining.pdf
[7] Araki M. “PID control”; Control systems, robotics, and Automation – Vol. II, ©Encyclopedia of Life Support Systems (EOLSS), at: http://www.eolss.net/ebooks/Sample%20Chapters/C18/E6-43-03-03.pdf
[8] Ziegler, J.G & Nichols, N. B. “Optimum settings for automatic controllers.” Transactions of the ASME. 64: 759–768, (1942).
[9] Nicolaus Allu, Apriana Toding. “Tuning with Ziegler Nichols Method for Design PID Controller At Rotate Speed DC Motor.” Study Program of Electrical Engineering Study Program, Faculty of Engineering;Universitas Kristen Indonesia Paulus (2020).
[10] Manoj kushwah , Ashish patra. “PID Controller Tuning using Ziegler-Nichols Method for Speed Control of DC Motor.” International Journal of Scientific Engineering and Technology Research; Volume.03, IssueNo.13 (June 2014). 2924-2929.
[11] Amruta S.Jondhale, Varsha J.Gaikwad, Satish R. Jondhale. “Level Control of Tank System using PID Controller-A Review.” IJSRD - International Journal for Scientific Research & Development, Vol. 3, Issue 10, 2015, ISSN (online): 2321-0613, 636-638
[12] Brenna M, Foiadelli F, Zaninelli Dj. “New stability analysis for tuning PI controller of power converters in railway application.” IEEE Transactions on ndustry Electronics (2011), 58 (2); 533-543.
[13] Manjurul Gani, Saiful Islam & Muhammad Ahsan Ullah. “Optimal PID tuning for controlling the temperature of electric furnace by genetic algorithm.” SN Applied Sciences; 1:880 | https://doi.org/10.1007/s42452-019-0929-y; © Springer Nature Switzerland AG (2019).
[14] S. Tamalouzt, Y. Belkhier, Y. Sahri, et al., "Enhanced Direct Reactive Power Control-Based Multi-Level Inverter for DFIGWind System under Variable Speeds," Sustainability, 13(16), 9060, 2021.
[15] Sittipong Pengpraderm, Kreangsuk Kraikitrat, Somporn Ruangsinchaiwanich. “Automatic control of synchronous motor using PI controller for improving power factor.” Journal of Thai Interdisciplinary Research; Volume 12, Number 5 (October 2017), 35 – 41.
[16] Maamoon F. Al-Kababji , Ahmed Nasser B. Al-Sammak. “Modeling & simulation of synchronous machine controlled by PID control for the reactive power compensation.” The 6th Jordanian International Electrical & Electronics Engineering conference JIEEEC (2005).
[17] Kennedy J, Eberhart R. “Particle swarm optimization.” Proceedings of the 1995 IEEE International Conference on Neural Networks, 4, Perth, WA (1995), Australia:1942-1948.
[18] W. Zeng, W. Zhu, T. Hui, L. Chen, J. Xie, and T. Yu, “An IMC-PID controller with Particle Swarm Optimization algorithm for MSBR core power control.”Nuclear Engineering and Design, 360, 110513, 2020.
[19] Jukka Kaukonen. “Slient pole synchronous machine modelling in an industrial direct torque controlled driver application.” Thesis for the degree of doctor of sience technology, Lappeenranta (1999); ISBN 951 – 764 – 305 – 5; ISSN 1456 – 4491.
[20] Bui Quoc Khanh, Doan Quang Vinh, Pham Quang Dang, Nguyen Quang Dich. “Industrial electric drive control.”; Scientific and technical Publishers (2020).